Available online at www.sciencedirect.com
SCIENCE DIRECT®
Electrochimica Acta 50 (2004) 1–10
ELECTROCHIMICA Acta
www.elsevier.com/locate/electacta

Effect of electrochemical polarization of PtRu/C catalysts on methanol electrooxidation

Gang Wu*, Li Li, Bo-Qing Xu

Department of Chemistry, Innovative Catalysis Program, Key Lab of Organic Optoelectronics and Molecular Engineering, Tsinghua University, Beijing 100084, China

Received 5 May 2004; received in revised form 2 July 2004; accepted 10 July 2004
Available online 14 August 2004

Abstract

To determine the influence of electrochemical polarization of PtRu/C catalysts on methanol electrooxidation, this work investigated methanol electrooxidation on as received and different electrochemically polarized PtRu/C catalysts. Thermogravimetric analysis (TGA) and X-ray diffraction (XRD) were used to characterize the redox state of PtRu/C after different electrochemical polarization. The methanol electrooxidation activity was measured by cyclic voltammetry (CV), Tafel steady state plot and electrochemical impedance spectroscopy (EIS). The results indicate that the metallic state Pt^0Ru^0 can be formed during cathodic polarization and contribute to electrooxidation of methanol, while the formation of inactive ruthenium oxides during anodic polarization cause the negative effect on methanol electrooxidation. Different Tafel slopes and impedance behaviors in different potential regions also reveal a change of the mechanism and rate-determining step in methanol electrooxidation with increasing potentials. The kinetic analysis from Tafel plots and EIS reveal that at low potentials indicate the splitting of the first C–H bond of CH_3OH molecule with the first electron transfer is rate-determining step. However, at higher potentials, the oxidation reaction of adsorbed intermediate CO_{ads} becomes rate-determining step.

Keywords: Methanol electrooxidation; PtRu/C catalyst; Electrochemical polarization; Tafel plot; Impedance spectroscopy

1. Introduction

Direct methanol fuel cell (DMFC) is more attractive as it removes the need for a fuel processor system and bypasses the handicap to store hydrogen as fuel [1–3]. Although the thermodynamic equilibrium potential of the electrooxidation of methanol is close to that of hydrogen oxidation, slow methanol electrooxidation rate is one of the major problems which decreases the conversion efficiency of chemical energy to electric energy. The half reaction is [4]:

$$CH_3OH + H_2O \rightarrow CO_2 + 6H^+ + 6e^-,$$
$$E^0 = 0.04\,\text{V versus RHE at } 25\,^\circ\text{C}$$

In acidic electrolytes only Pt and Pt-based catalysts have been shown to give useful rates for methanol oxidation. Since it is unlikely that these six electrons can be transferred simultaneously, this leads to the formation of surface adsorbed intermediate species, which could act as poisons for subsequent methanol adsorption and oxidation. It is generally accepted that the methanol can be oxidized to CO_2 via a CO or $HCOO^-$ reactive intermediates and the formation of strongly adsorbed linearly bonded CO leads to the self-poisoning of Pt electrocatalysts. Adsorption of methanol on poisoned Pt cannot occur, and hence methanol oxidation drops to an insignificant rate [5–7].

It is known from investigations of Gasteiger et al. [8] and Tseung et al. [9] that Ru, Sn, W and Mo exhibit co-catalytic activity with Pt for the anodic oxidation of methanol due to the lower potential required for the dissociation of water and providing of OH_{ads} species on these elements, thereby

* Corresponding author. Tel.: +86 10 62795834; fax: +86 10 62792122.
E-mail address: wugang1976@hotmail.com (G. Wu).

0013-4686/$ – see front matter © 2004 Elsevier Ltd. All rights reserved
doi:10.1016/j.electacta.2004.07.006

allowing more facile oxidation of the carbonaceous adsorbate on adjacent Pt sites. However, there are several practical factors limiting the choice of these metals. Many O-adsorbing metals can produce negative effects, e.g. inhibit methanol adsorption or may be not sufficiently stable for long-term use in acid media. At present PtRu offers the most promising results for methanol oxidation. Most of the literature data [10–12] agree that the onset of the methanol oxidation reaction on PtRu catalyst is about 0.2–0.3 V less positive than on the single Pt catalyst. The effect of Ru is usually assumed to follow a so-called bifunctional mechanism originally suggested by Watanabe and Motoo [13] and Ligand model [14,15], which is based on the modification of Pt electronic structure by the presence of Ru, cause a weak chemisorption bond of CO_{ads} to the Pt–Ru alloy with respect to pure Pt.

Presently, binary PtRu catalysts for methanol oxidation are studied by diverse forms, for example, PtRu alloys [16,17], Pt + Ru/C [18], Ru electrodeposits on Pt [19], PtRu codeposites [20,21] and Ru adsorbed on Pt [22,23].

However, at present, whether an alloy structure or metallic form even or combination of oxide and metal is more contribution to methanol electrooxidation is still in debate.

Early work revealed that Pt/Ru alloys have a unique activity for the electrooxidation of methanol [16,17]. The decrease of the lattice parameters in the presence of Ru does support to the idea that PtRu/C catalysts are a solid solution of Pt and Ru, rather than a physical mixture of particles of two metals [24]. In general, alloying two metals can alter their electronic structure as well as their geometric structure. It has been shown that the metal-adsorbate bond strength on the alloy surface can be very different from that on the pure metal surfaces and can therefore alter the mechanism of a reaction [25]. Tong et al. [26] studied the correlation between the $2\pi^*$ Fermi level local density of states and the steady-state current and suggested a role for Ru in weakening the Pt–CO bond, thereby increasing the CO oxidation rate. The similar results also obtained from Ge et al. [27], they revealed that Pt–CO bond was weakened from 1.54 to 1.36 eV after Ru alloying with Pt for the bulk Pt–Ru alloy. Using clusters consisting of 10 metal atoms, Liao and co-workers [28,29] found that the presence of Ru metal atom weakens the Pt–C bond and slightly lowers the C–O stretching frequency of CO. Mallouk and co-workers [30] investigated the Pt–Ru–Os–Ir quaternary alloy catalyst, in light of phase equilibrium between M–C and M–O bond strengths. The composition of the best quaternary catalysts is in accord with estimates of the maximum solubility of the alloying elements in f.c.c. Pt. This result implies that earlier steps in the methanol electrooxidation mechanism involve C–H bond activation and the role of alloy element is to accelerate these processes.

However, in recently, several papers [31–33] indicated an alloy structure is not a prerequisite for obtaining the highest activity and the practical PtRu/C catalyst are not single phase materials, but are instead bulk mixtures of Pt metal, Pt hydrous oxides, and hydrous and dehydrated RuO_2, only a minor fraction (25%) of the Ru is present as metal. Rolison [31,32] indicated that the presence of hydrous ruthenium oxide phase (RuO_xH_y or $RuO_2{\cdot}xH_2O$) in practical PtRu/C catalysts has important mechanistic implications for methanol oxidation because RuO_xH_y is mixed III/IV valent and conducts both electrons and protons and also efficiently dissociates H_2O. The RuO_xH_y speciation of Ru in nanoscale PtRu blacks affords a much more active catalyst for methanol oxidation than Ru^0 does as part of a bimetallic alloy.

But opposite results from Hoster et al. [34] had indicated that at a constant potential of 0.5 V, a pronounced initial loss of activity for methanol electrooxidation on smooth PtRu materials seem to be caused by the oxidation of the Ru surface forming oxides like RuO and RuO_2, which are not active as oxygen donors for CO_{ads} oxidation. The electrode activity is thus partially recovered by applying a potential step toward more negative values, where the Ru oxide species are reduced. Birss and co-workers [33] treated the PtRu/C catalysts either in hydrogen or oxygen at elevated temperature to alter the oxidation state. The methanol oxidation activity was measured and the sequence at 25 °C was found to be reduced > as-received > oxidized ≫ strongly oxidized. Furthermore, by using X-ray absorption near edge structure (XANES) [35] studies, it is clear that PtRu/C catalysts are predominately oxides as prepared state. However, after they are introduced into an electrochemical cell at the potentials where methanol oxidation occurs, they are reduced to the metallic state. The above results seem to means the metallic state Pt^0Ru^0 is more active to methanol oxidation than Ru oxides.

So it can be seen that the effect of surface redox state of PtRu/C on methanol electrooxidation is still ambiguous. In this work, we consider the fact that the chemical states of Pt and Ru in nanoscale PtRu/C catalysts can be manipulated by electrochemical polarization. Electroanalytical studies confirm that the surface of Ru metal oxidizes at room temperature to a mixed-valent Ru^{III}/Ru^{IV} oxide in acid electrolyte at 0.2–0.4 V versus normal hydrogen electrode (NHE) [36]. So the metallic form Pt^0Ru^0 can be formed under the specific condition of cathodic polarization, while a mixed-phase electrocatalyst containing Pt^0 and Ru oxides also can be formed under specific potential by anodic polarization. Different surface chemical state of Pt and Ru in PtRu/C catalysts caused by different electrochemically polarized maybe affect the reaction activity of methanol electrooxidation.

The primary goal of the present work is attempting to understand the relationship between well-characterized electrochemical polarization and relative methanol electrooxidation activity on PtRu/C catalysts. Different electrochemically polarized catalysts were characterized using, thermogravimetric analysis (TGA), and X-ray diffraction (XRD), cyclic voltammetry (CV), Tafel plot and electrochemistry impedance spectroscopy (EIS) to confirm the correlation between redox states of PtRu/C and their oxidation activity. EIS is a powerful tool to investigate the electron transfer in electrochemical reaction. Melnick et al. [37,38] had revealed the impedance behavior of methanol electrooxidation on polished polycrystalline Pt to explain the effect of surface coverage of

intermediates on reaction mechanism. But, until now, the impedance investigation on PtRu/C catalyst is still scanty. The kinetic data of methanol electrooxidation by Tafel slopes and EIS are presented in this work also. The balance between the initial dehydrogenation of methanol and the oxidative removal of the intermediates has a major influence on the reaction kinetics.

2. Experimental

2.1. Electrochemical pretreatment of the catalyst

The PtRu/C catalysts (Johnson Matthey catalysts 40 mass% metal loading, Pt:Ru = 1:1 atom ratio) were used in the experiments. Five percent Nafion isopropanol solution was used to disperse catalysts. This solution was sonicated for 30 min and then the catalyst suspending solutions were applied by micropipet to the glassy carbon (GC) electrode surface, with a given catalyst loading of 3.2 mg cm^{-2}. After the catalysts were applied to the GC electrode, they were air-dried for 30 min at 60 °C. Then the PtRu/C catalysts deposited on GC electrode were studied in three forms: as received, cathodically polarized and anodically polarized. Cathodic polarization was carried out under the −0.30 V for 2 h at 25 °C in 0.5 M H_2SO_4 solution. Anodic polarization also achieved under 0.55 V for 2 h. Higher anodic potential maybe cause Pt oxidation and form the dissolved oxide RuO_4.

2.2. Catalyst characterization

Thermogravimetric analysis was carried out using a TA Instruments Mettler TGA/SDTA 851 to determine the extent of oxidation of the different polarized PtRu/C catalysts. The effect of carbon support was corrected from the blank TGA of Vulcan XC-72. Different samples weighing 5–10 mg were loaded into alumina pans and heated from 50 to 650 °C at 10 °C min^{-1} under air at a flow rate of 20 mL min^{-1}.

XRD analysis was carried out on a Bruker d8 diffractometer system equipped with a Cu Kα radiation and a graphite monochromatic operationg at 45 kV and 40 mA. The patterns were obtained at a scan rate of 5° min^{-1} with step of 0.02°.

2.3. Electrochemical measurement

A conventional three-electrode test cell was used. The working electrode was electrochemically polarized PtRu/C deposited on rotation disc GC electrode held in a Teflon cylinder at 500 rpm. A Pt gauze and a saturated calomel electrode (SCE) were used as counter and reference electrodes, respectively. All potentials in this paper are quoted against normal hydrogen electrode. Cyclic voltammogram (CV) and Tafel polarization curves were executed with an EG&G model 273 potentiostat/galvanostat. Electrochemical impedance spectroscopy was measured by a Solarton 1255 frequency response analyzer and the frequency ranged from 100 kHz to 0.01 Hz. The sweep rate in CV measurement is 20 mV s^{-1} and in Tafel plot is 0.1 mV s^{-1}. CV and EIS were carried out at room temperature (23 ± 2 °C), and Tafel polarization curves were measured at different temperatures: 23, 40, 60 and 70 °C. For methanol electrooxidation, the solution was 0.5 M CH_3OH in 0.5 M H_2SO_4, which prepared from high purity sulfuric acid, methanol and double distilled water. All electrolyte solutions were purged by high purity N_2 for 1 h prior to any measurements.

In order to evaluate the effect of mass transport, assuming a diffusion coefficient of CH_3OH, D_i of 1.3×10^{-5} cm^2 s^{-1}, a viscosity of solution ν of ca. 1.0, 500 rpm rotating rate and methanol concentration C_i, 0.5 M, so the limitation current densities can be approximately calculated and given as follows:

$$j_d = 0.62nFD_i^{2/3}\omega^{1/2}\nu^{-1/6}C_i \approx 150\,\text{mA}\,\text{cm}^{-2}$$

So the limitation current densities, j_d is more larger than the current densities of methanol electrooxidation (about 20 mA cm^{-2}), so the mass transport limitation can be completely ignored.

3. Results and discussion

3.1. Thermogravimetric analysis of catalysts

Fig. 1 shows the TGA curves of the PtRu/C after different electrochemical treatment (as received, cathodically polarized and anodically polarized). Since the measurements were made in flowing dry air, the sample weight gain on the TGA curve should means an oxidation of metallic or low valent oxide component in catalysts. All of samples exhibit a small initial decrease in mass, likely due to a loss of water. The cathodically polarized sample demonstrates a weight increase in mass at 200–500 °C, probably reflecting oxide formation, suggesting that the cathodically polarized PtRu may exist as the metallic state of Pt^0Ru^0. If all of the Pt in these catalyst

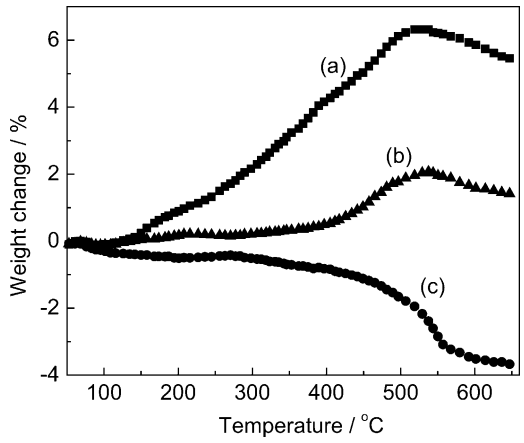

Fig. 1. Themogravimetric analysis of (a) cathodically polarized, (b) as received and (c) anodically polarized PtRu/C catalysts.

were oxidized to PtO and PtO_2, this would give a 5.4% mass gain of the entire sample, while oxidizing both Ru and Pt to RuO and PtO would result in a 9.7% mass gain [32]. The total mass gain for the reduced sample was approximately 6.7% consistent with these predictions. However, the as received sample shows a mass gain at 400–500 °C. This may be form oxidation containing more oxygen. The initial loss mass of anodically polarized PtRu catalyst below 200 °C maybe is structure water from hydrous oxide phases and no longer evident for cathodically polarized and as received. Furthermore, the anodically polarized sample shows almost no dominant mass gain, between 100 and 500 °C, indicating that the sample was already oxided and could not undergo any further oxidation. The decrease in mass between 500 and 650 °C, seen in all samples may be due to PtO_xH_y species decomposing to Pt [33].

3.2. XRD analysis

The XRD patterns of all samples are shown in Fig. 2 and reveal f.c.c. crystal structure of metallic Pt. Vertical lines on the diagram represent position of the peaks of pure Pt, PtO and RuO_2. Only the anodically polarized PtRu/C catalyst exhibits oxidized phase of RuO_2 and PtO, consistent with the features observed in the TG. Moreover, it can be seen that all peaks of PtRu catalyst are shifted towards higher angles comparing to pure Pt, suggesting that a part of Ru existence was alloyed with Pt in commercial PtRu/C catalyst (John Matthew).

3.3. CV characteristic

CV is probably the most widely used technique for the electrochemical characterization of electrocatalysts. Fig. 3 shows the CV for different electrochemically polarized and as received PtRu/C in nitrogen purged 0.5 M H_2SO_4 at 25 °C. The potential range from 0 to 0.9 V can be divided into three regions. The low potential region (0–0.35 V) covers H adsorption and desorption region. The intermediate potential region (0.35–0.6 V) corresponds to the double layer region

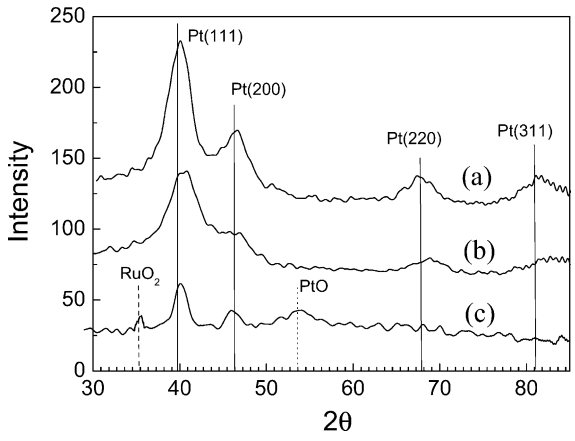

Fig. 2. XRD pattern of PtRu/C, 40 mass% metal loading, Pt:Ru = 1:1 atom ratio: (a) cathodically polarized; (b) as received; (c) anodically polarized.

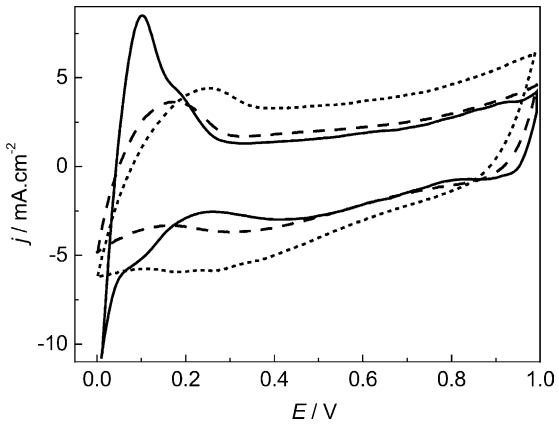

Fig. 3. Cyclic voltammograms of 40 mass% PtRu/C catalysts in 0.5 M H_2SO_4 solutions, sweep rate 20 mV s^{-1}. cathodic polarization (—); as received (------); anodically polarized (. . . . .).

of PtRu/C and the high potential region refers to potentials above 0.6 V. The voltammetric responses of different polarized and as received PtRu/C catalysts corroborate various Ru chemical states. From literature [32,39,40], in the case of Ru metal, hydrogen adsorption/desorption peaks in CV were seen centered at 0.1 V, anodic current due to compact Ru oxide formation was also seen, commencing already at 0.3 V. Hydrous Ru oxide displays large preudocapacitive currents throughout the potential range.

From the CV feature of electrochemically polarized PtRu/C catalysts, one striking difference can be seen in the hydrogen adsorption and desorption region, where cathodically polarized catalyst displays a marked hydrogen adsorption–desorption current at 0.05–0.25 V in contrast to anodically polarized and as received catalysts. This catalyst may have a high percentage for Pt^0 and Ru^0 in catalyst surface to adsorb H easily after cathodic polarization. Iwasita et al. [22] had reported that the PtRu/C catalyst prepared via reduction with H_2 exhibit a sharp peak at ca. 0.1 V. This feature has been related to hydrogen desorption from Ru islands around the Pt metal. Meanwhile, cathodically polarized PtRu/C shows only small currents in the double-layer region, while high current in the double layer region is observed in the voltammograms of anodically polarized PtRu catalyst. This is ascribed to the adsorption of oxygen-containing species on Ru oxides.

So, by comparing the CV responses for metallic Pt and Ru and for hydrous Ru oxide with different polarized PtRu/C catalysts, the anodically polarized PtRu/C catalyst shows the more capacitive features of Ru oxide, while the cathodically polarized PtRu sample displays more distinct H peak region, typical of the metallic Pt^0 and Ru^0 states.

3.4. Methanol electrooxidation

3.4.1. Cyclic voltammetry for methanol electrooxidation

In order to determine methanol oxidation activity of the as received, cathodically polarized and anodically polarized

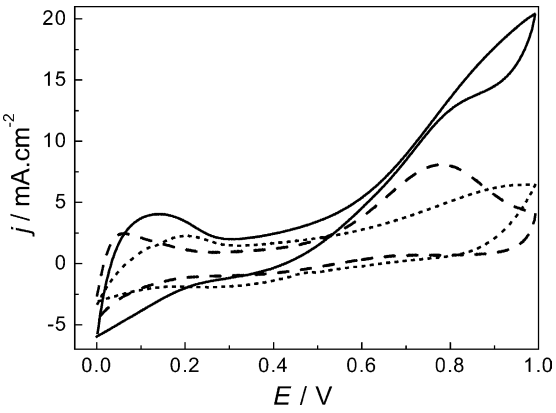

Fig. 4. Cyclic voltammetry of methanol electrooxidation on different electrochemically polarized PtRu/C catalyst in 0.5 M CH_3OH + 0.5 M H_2SO_4 solutions, sweep rate 20 mV s^{-1}. Cathodically polarized (—); as received (- - - - -); anodically polarized (. . .. . .).

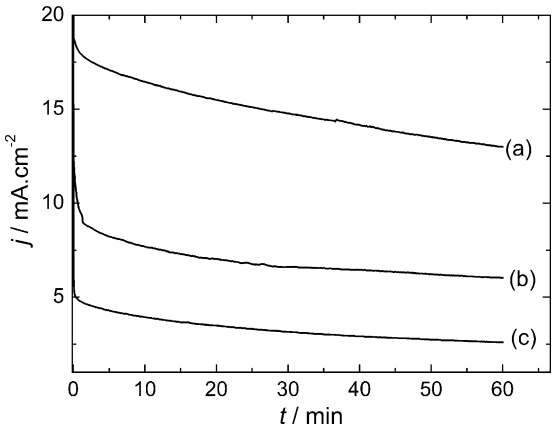

Fig. 5. Current–time curves at 0.55 V for different electrochemically polarized PtRu/C catalysts, 0.5 M CH_3OH + 0.5 M H_2SO_4, room temperature: (a) cathodically polarized; (b) as received; (c) anodically polarized.

PtRu/C catalysts, the CV of these samples in 0.5 M methanol in 0.5 M H_2SO_4 solution, sweep rate of 50 mV s^{-1}, room temperature and 500 rpm were investigated and shown in Fig. 4. The oxidation activity on cathodically polarized PtRu/C catalyst is much higher than any other samples, and followed by the as received and then the anodically polarized sample. This result is consistent with extended X-ray absorption fine structure (EXAFS) data [41] showing the metallic PtRu catalyst is stable under fuel cell operation. A low activity of methanol electrooxidation on anodically polarized PtRu/C catalyst might be caused by formation of surface Ru oxides that are not electrochemically active, i.e. the simply act to block the surface and cannot be electrochemically reduced during the methanol oxidation.

Furthermore, for cathodically polarized sample, the reverse scan during methanol oxidation yields slightly lower currents than during the forward scan, while the deactivation of methanol electrooxidation on as received and anodically polarized samples is obviously visible in reverse scan. A reasonable explanation of a loss in activity is adsorption of poisoning species on electrode surface. During methanol oxidation reaction at PtRu/C, the intermediates accumulate on the surface blocking active sites for further oxidation. Briss and co-workers [33] had revealed that the current measured in the reverse scan can be assumed to be actual activity of methanol electrooxidation and was therefore used to compare the methanol oxidation activity of the various catalysts in this work.

3.4.2. Current–time curves for methanol electrooxidation

Fig. 5 shows typical current–time responses for methanol oxidation at 0.55 V on different electrochemically polarized PtRu/C catalysts. As expected, the methanol oxidation current at cathodically polarized PtRu/C is higher than that of as received and anodically polarized samples. Meanwhile, the PtRu/C sample after anodic polarization is less active than the as received sample.

All sample present a current decay in current–time measurements, which was also observed for smooth UHV prepared PtRu sample [34]. Moreover, the most interesting feature deserving our attention is that the current–time curves measured on the anodically polarization PtRu/C electrode exhibits less decay than others. The difference in behavior of initial decay of methanol electrooxidation current on different electrochemically polarized PtRu/C materials is probably related to the surface redox state. According to Hoster et al. [34], the possible origin of the initial decay in methanol electrooxidation can be related to the formation of some Ru oxide. Because the cathodic polarization may cause metallic Ru and some oxide would be formed during initial methanol electrooxidation so the initial loss of activity is evident. However, some Ru oxides have already formed on sample surface after anodic polarization, the initial activity loss due to formation of Ru oxide on anodically polarized sample is not so obviously. It can be found from current–time curves that the formation of Ru oxides can be considered as an inhibiting factor for methanol electrooxidation, responsible for the initial deactivation process.

3.4.3. Tafel curves

In our experiments, the methanol oxidation activity was clearly related to the condition of electrochemical polarization. This relationship is investigated further by measuring the kinetic parameters. Tafel slope and exchange current density is two fundamental kinetic parameters in electrochemical reactions.

Tafel plots of different electrochemically polarized PtRu/C catalysts at temperatures of 40 and 70 °C are shown in Fig. 6. All polarization curves were corrected for ohmic drop effects, with resistance values obtained from impedance measurements. Among the three samples, the cathodically polarized PtRu/C catalyst shows the highest activity for methanol electrooxidation. Moreover, these Tafel plots can be fitted and divided into two linear regions that intersect at approximately 0.55 V for all samples, indicating a change in the

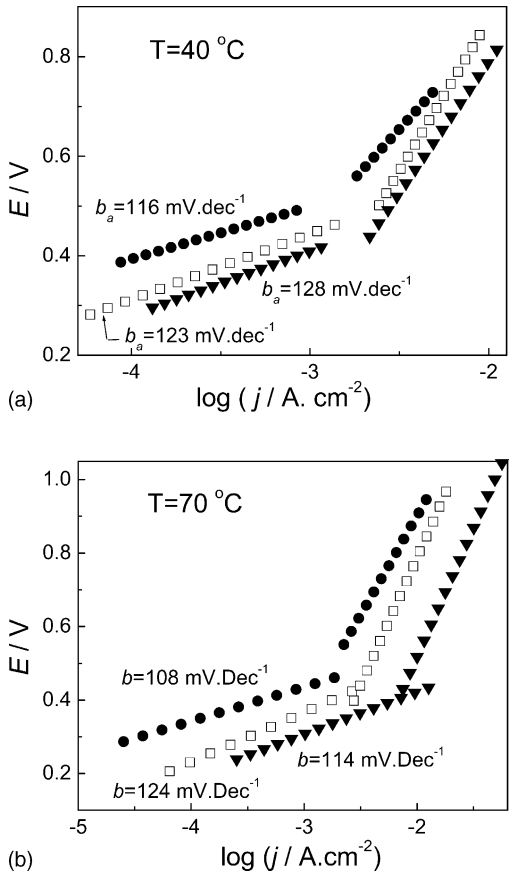

Fig. 6. Tafel plots for methanol electrooxidation on different electrochemically polarized PtRu/C catalyst in 0.5 M CH_3OH + 0.5 M H_2SO_4 solutions at different temperature (a) 40 °C, (b) 70 °C; cathodically polarized (▼), as received (□), anodically polarized (●).

mechanism or at least a change in the predominance of certain processes. Although the linear region is not wide enough in all cases, at all temperatures the fitted Tafel slopes are about 108–128 mV dec^{-1} at low potentials (below 0.55 V) and are about 300–700 mV dec^{-1} at high potentials (above 0.55 V).

Due to rather similar Tafel slopes of about 118 mV dec^{-1} in the low potential region, electrochemical behaviors for all three samples are almost identical. From the kinetic theory of electrode reaction, Tafel slopes of about 118 mV dec^{-1} means that the unit reaction involving the first electron transfer is rate-determining step. So it can be concluded that a splitting of the first C–H bond of CH_3OH molecule with the first electron transfer is rate-determining step of methanol electrooxidation on various PtRu/C at the low potentials. In situ infrared reflectance spectroscopy measurements by Dubau et al. [42] also suggest at potential range of 0.34–0.40 V, the CO diffusion on Pt is very fast, and the reaction between adsorbed CO and adsorbed OH is also very fast, so methanol dehydrogenation is the rate-determining step of methanol oxidation on Pt + Ru/C catalyst.

However, with an increase of potential, Tafel slopes in the range of 300–700 mV dec^{-1} at high potentials indicates that rate-determining step is changed. Reaction between adsorbed CO on Pt sites and OH species on Ru sites were hypothesized to be rate-determining step. The further proofs were given at succeeding EIS measurements.

3.4.4. *Influence of temperature*

To evaluate the temperature dependence of methanol oxidation on different PtRu/C catalysts, Tafel plots were measured in 0.5 M methanol in 0.5 M H_2SO_4 solutions at 23, 40, 60 and 70 °C. Fig. 6 also shows that at low potentials, the Tafel slopes of all samples seem independent on temperature, while at high potentials, slopes increased with an increase of temperature. A reasonable explanation might be that temperature has no influence on the mechanism of methanol dehydrogenation on Pt sites but can change the pathway of oxidation of adsorbed CO_{ads} and –HCOO. However, a more detailed kinetic interpretation of the results is difficult, as the electrocatalytic oxidation of methanol is a very complex reaction involving the transfer of six electrons. Arrhenius plots of exchange current density $\log j_0$ obtained from low potentials versus $1/T$ are given in Fig. 7, which activation energies were estimated from these slopes of linear fitted. The activation energy of methanol electrooxidation on cathodically polarized PtRu/C is about 62.5 kJ mol^{-1} and has the lowest value among the three samples (as received and anodically polarized PtRu/C are 68.2 and 74.6 kJ mol^{-1}, respectively). These values are very closed to 65 kJ mol^{-1} [43] that was determined on PtRu/C prepared by E-Tek with 40 mass% metal loading and Pt:Ru = 1:1 alloy, but higher than the value of 35 kJ mol^{-1} reported for methanol oxidation on Pt + Ru/C catalyst [44].

3.4.5. *Electrochemical impedance spectroscopy for methanol electrooxidation*

In order to further compare the activity of methanol electrooxidation on the different electrochemically polarized PtRu/C catalysts and to investigate mechanism information, EIS were carried out at different potentials. Fig. 8 shows

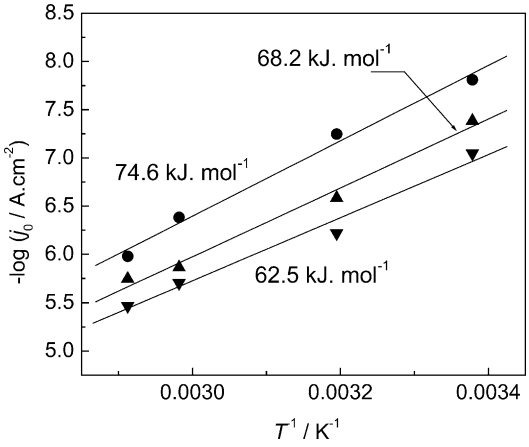

Fig. 7. Exchange current density, j_0 of Methanol electrooxidation on different electrochemically polarized PtRu/C catalyst as a function of temperature in 0.5 M CH_3OH + 0.5 M H_2SO_4 solutions: cathodically polarized (▼), as received (▲), anodically polarized (●).

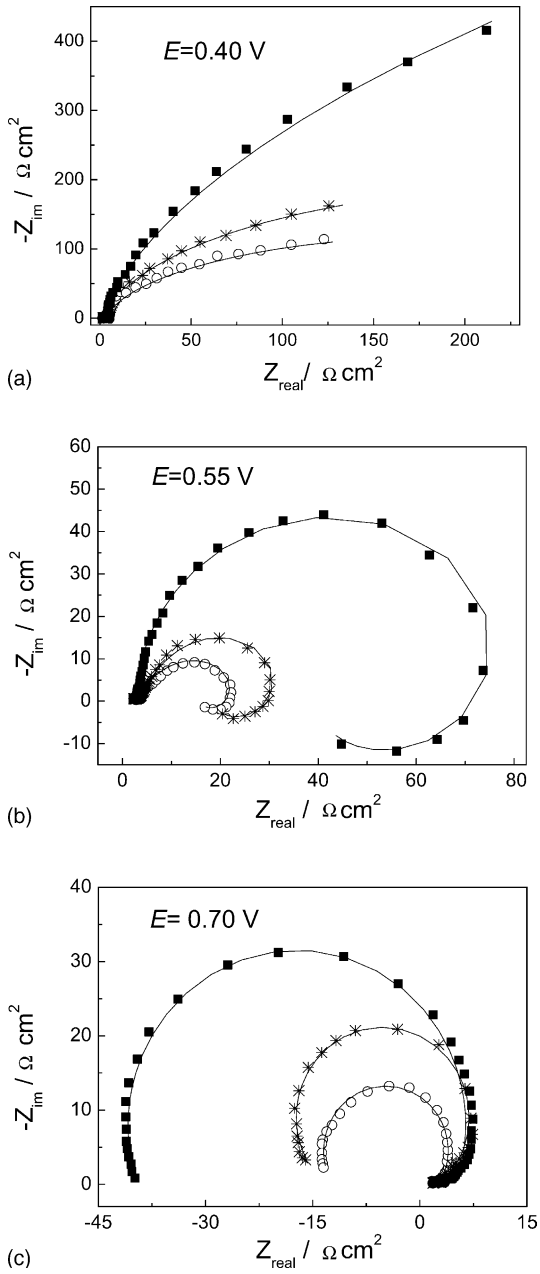

Fig. 8. Nyquist plots of EIS for methanol electrooxidation on different electrochemically polarized PtRu/C catalysts: cathodically polarized (◯), as received (✳), anodically polarized (■), simulated values (—), at different potential: (a) 0.40 V; (b) 0.55 V; (c) 0.70 V.

Nyquist plots of the impedance of methanol electrooxidation on different electrochemically polarized PtRu/C catalysts at potentials of 0.40, 0.55 and 0.70 V.

The EIS results indicate that the methanol electrooxidation on PtRu/C catalysts at various potentials shows different impedance behaviors. In order to analyze reaction mechanism of methanol electrooxidation on PtRu/C catalysts, a simple two-step model for methanol electrooxidation can be assumed:

$$CH_3OH \xrightarrow{I_1} CO_{ads} + 4H^+ + 4e^- \quad (1)$$

$$CO_{ads} + H_2O \xrightarrow{I_2} CO_2 + 2H^- + 2e^- \quad (2)$$

According to the bifunctional mechanism of methanol electrooxidation on PtRu catalyst [13], methanol is adsorbed mainly on Pt sites, while OH is come from dissociation of H_2O on Ru sites. I_1 is the rate leading to the adsorbed surface intermediates CO_{ads}. I_2 is the rate for oxidation of CO_{ads}. Since mass transport limitation is assumed can be ignored with the rotating disc electrode. I_F is the Faradaic current and stand for net rate of charge transfer. In this assuming, we just consider only one intermediate CO_{ads} in methanol electrooxidation.

$$I_1 = k_1 c_m (1 - \theta_{CO}) \quad (3)$$

$$I_2 = k_2 \theta_{CO} \theta_{OH}, \qquad I_F = I_1 + I_2 \quad (4)$$

where θ_{CO} and θ_{OH} are the fractional surface coverage of CO_{ads} and OH, respectively. For simplifying the analysis, the variation of θ_{OH} is assumed to have little effect on impedance behavior of methanol electrooxidation, defined as

$$\Theta = \frac{d\theta}{dt} = \frac{F}{q_{CO}}(I_1 - I_2) = K(I_1 - I_2)$$

where q_{co} is the quantity of charge needed to complete a full coverage of CO on the electrocatalyst.

According to the kinetic theory derived by Harrington and Conway [45] and Cao [46] for reactions involving intermediate adsorbate, in the electrode process of methanol electrooxidation, the Faradaic current depends on the electrode potential E and one other state variable θ_{CO} varying with E and affecting the Faradaic current.

So the Faradaic admittance of methanol electrooxidation is

$$Y_F = \frac{1}{R_{ct}} + \frac{B}{a + j\omega} \quad (5)$$

where $R_{ct} = (\partial E/\partial I_F)_{ss}$ is charge transfer resistance of the electrode reaction and is the only circuit element that has a simple physical meaning describing how fast the rate of charge transfer during methanol electrooxidation changes with changing electrode potential when the surface coverage of the intermediate is held constant. The subscript "ss" denotes steady state. R_{ct} also can be defined as $R_{ct} = \lim_{\omega \to 0} Re\{Z_f\}$ where $\mathrm{Re}\{Z_f\}$ is the real component in complex plots (Nyquist plots), ω the circular frequency $\omega = 2\pi f$. So R_{ct} can be obtained directly from Nyquist plots.

In spite of the different impedance behaviors (Fig. 8) at different potentials, from cathodically polarized PtRu/C catalyst to as received, then to anodically polarized, the diameter of the primary semicircle meaning the value of R_{ct} increases. The results indicate that reaction activity of methanol electrooxidation is positively affected by the cathodic polarization but it is negatively affected by the anodic polarization.

In Eq. (5), $a = -(\partial\Theta/\partial\theta)_{ss} > 0$ a is the always positive for a stable steady process and with a dimension of s^{-1}, defined as $B = mb$ where $m = \partial I_F/\partial\theta$, $b = (\partial\Theta/\partial E)_{ss} = d\theta/dE$, and B with dimensions of $\Omega^{-1}\,cm^{-2}\,s^{-1}$.

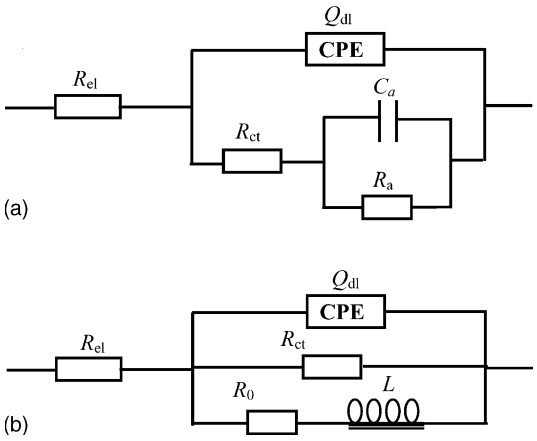

Fig. 9. Electrical equivalent circuit used for simulating the impedance spectra for the methanol electrooxidation on PtRu/C catalyst at different potentials: (a) at 0.4 and 0.7 V, (b) at 0.55 V.

The impedance Nyquist plots can be classified according to the sign of B value.

When $B > 0$, Eq. (5) can be rewritten as follows:

$$Y_F = \frac{1}{R_{ct}} + \frac{1}{a/B + j\omega/B} = \frac{1}{R_{ct}} + \frac{1}{R_0 + j\omega L} \tag{6}$$

The dimension of R_0 is $\Omega\,cm^2$ and of L H cm^2. Thus there will be an inductive component involved in Faradaic impedance. The equivalent circuit of the impedance based in Eq. (6) is shown in Fig. 9(b). The Faradaic branch of this circuit consists of a resistor R_{ct} parallel with a series of a resistor R_0 and inductance L. The impedance Nyquist plot will be a capacitive arc in the high frequency range and an inductive arc in the low frequency range.

When $B < 0$, in this case:

$$Y_F = \frac{1}{R_{ct}} - \frac{|B|}{a + j\omega}$$

The Faradaic impedance can be rewritten as

$$Z_F = \frac{1}{Y_F} = R_{ct} + \frac{{R_{ct}}^2|B|}{a - R_{ct}|B| + j\omega}$$
$$= R_{ct} + \frac{R_a}{1 + j\omega R_a C_a} \tag{7}$$

with $R_a = {R_{ct}}^2|B|/a - R_{ct}|B|$, $C_a = 1/{R_{ct}}^2|B|$.

The dimension of R_a is $\Omega\,cm^2$ and of C_a, F cm^{-2}. Thus the equivalent circuit of the impedance based in Eq. (7) is as shown in Fig. 9(a). The Faradaic branch of this circuit consists of a resistor, R_{ct} in series with a parallel combination of a resistor, R_a and capacitor, C_a. Furthermore, in this group there are still two cases, which can be classified.

When $a - R_{ct}|B| > 0$, then $R_a > 0$, two capacitive arcs will be displayed on the first quadrant of Nyquist plot. When $a - R_{ct}|B| < 0$, then in this case $R_a < 0$, and the capacitive arc in low frequency range will enter into the second quadrant of Nyquist plot.

To obtain a satisfactory impedance simulation of methanol electrooxidation, it is necessary to replace the double layer capacitor, C_{dl} with a constant phase element (CPE) Q_{dl} in equivalent circuit. The most widely accepted explanation for the presence of CPE behavior and depressed semicircles on solid electrodes is microscopic roughness, causing an inhomogeneous distribution in the solution resistance as well as in the double-layer capacitance [47].

According to above analysis, for methanol electrooxidation on PtRu/C catalysts, the impedance parameters from Eqs. (3) and (4) can be deduced and are as follows:

$$b = \left(\frac{\partial\Theta}{\partial E}\right)_{ss} = \frac{\partial[K(I_1 - I_2)]}{\partial E}$$
$$= K\frac{\alpha F}{RT}[k_1 c_m(1 - \theta_{CO}) - k_2\theta_{CO}\theta_{OH}]$$
$$= K\frac{\alpha F}{RT}[k_1 c_m - (k_1 c_m + k_2\theta_{OH})\theta_{CO}] \tag{8}$$

$$m = \left(\frac{\partial I_F}{\partial\theta}\right)_{ss} = \frac{\partial(I_1 - I_2)}{\partial\theta} = k_2\theta_{OH} - k_1 c_m \tag{9}$$

So the impedance behaviors of methanol electrooxidation in different potential ranges can be discussed as follow and the simulated results were shown as solid line also in Fig. 8.

(1) When methanol electrooxidation at low potential range (0.4 V), assumes reaction (1), methanol dehydrogenation is rate-determining step, then $k_1 \ll k_2$.

So, when $k_2\theta_{OH} > k_1 c_m$, According to Eqs. (8) and (9), thus $b < 0$, and $m > 0$, namely $B < 0$.

From Eq. (7), Nyquist plots of EIS at 0.4 V should show capacitive behaviors. Moreover, in this case, $a - R_{ct}|B| > 0$, so two overlapped capacitive semicircles should exist in Nyquist plot and signify a reaction with one adsorbed intermediate. The EIS data can be simulated using the equivalent circuit Fig. 9(a). These theoretical analyses have a good agreement with our experimental results (shown in Fig. 8(a)). So the assumption that methanol dehydrogenation is rate-determining step should be reasonable.

On the other hand, Tafel slopes of the methanol electrooxidation from Fig. 6 are about 118 mV dec^{-1} at 0.4 V for all samples, indicating that the rate-determining step is the first electron process. So, these analyses from EIS and Tafel slopes indicate that, at low potential region, reaction (1) might be rate-determining step, and means the oxidation of CO_{ads} with the OH_{ads} on Ru sites is fast.

(2) When methanol electrooxidation at intermediate potential range (0.55 V), with an increase of potential, the rate of reaction (1) is increasing, but is not enough to exceed the rate of reaction (2) obviously. So in this case the rate-determining step of methanol electrooxidation is in transition region.

Thus maybe has following relationship:

$$k_2\theta_{OH}\theta_{CO} + k_1 c_m\theta_{CO} > k_1 c_m > k_2\theta_{OH}$$

From Eqs. (8) and (9), $b < 0$, and $m < 0$ can be deduced and then $B = mb > 0$.

According to Eq. (6) an inductive arc in low frequency range will be exhibited in Nyquist plot. The inductive behavior from theoretical analysis is also observed in our experiments shown in Fig. 8(b). The EIS data can be simulated using the equivalent circuit Fig. 9(b). In general, the condition of occurrence of an inductive behavior in Nyquist plot is $mb > 0$. This means, if the variation of the electrode potential causes a variation of the Faradaic current density not only through its effect on the strength of the electric field in the double layer but also through its effect on another variable X and the both effects act in the same direction, an inductive component will be involved in the Faradaic impedance [46]. According to impedance parameters, b and m, inductive behavior in methanol electrooxidation reveals the CO_{ads} coverage decreases with increasing potential ($b < 0$), and the decreasing CO_{ads} lead to an increase of Faradaic current ($m < 0$). A reasonable explanation is with potential increasing, the large amounts of OH_{ads} are formed on Ru sites and react with CO_{ads} and decrease its coverage. Meanwhile, the decreasing surface coverage of CO_{ads} will contribute to adsorption of methanol on Pt and enhance the Faradaic current. So at the intermediate potential range, with an increase of potential from 0.4 to 0.55 V, the transition from capacitive behavior to inductive behavior indicates that the rate-determining step maybe is changing. The results from EIS are consistent with analyses from Tafel slopes that are transforming from about 118 mV dec^{-1} to higher values. Moreover, the similar inductive behavior in EIS at about 0.55 V is also observed recently at the anode of a DMFC [48].

(3) When methanol electrooxidation at high potential range (0.70 V), in this case, reaction (2) can be assumed as rate-determining step.

Thus, $k_1 \gg k_2$ and then $k_2\theta_{OH} < k_1 c_m$.

According to Eqs. (8) and (9), $b > 0$ and $m < 0$ can be deduced, then $B < 0$.

Moreover, in this case $a - R_{ct}|B| < 0$. The capacitive arc at low frequency in Nyquist plot will flips to the second quadrant with the real component of the impedance becoming negative. The theoretical analyses agree well with the experimental results shown in Fig. 8(c). The EIS data can also be simulated using the equivalent circuit Fig. 9(a). This means that resistance R_a becomes negative resulting from passivation of electrode surface [49]. Melnick et al [38] indicated that the passivation of the Pt electrode during methanol electrooxidation is probably due to the reversible formation of oxide species. Meanwhile, due to reaction (2) is rate-determining step, the oxidation of CO_{ads} with OH is very slow, so the passivation at higher potentials can be explained by the formation of a large amount of CO_{ads} and OH on surface of PtRu catalyst. Therefore, adsorption of methanol on Pt sites is inhibited due to an increase of coverage of CO_{ads} and OH on Pt sites and the electrooxidation rate is almost no obvious increase. Moreover, from Tafel plots, at high potential region, it also can be seen that the current density is almost no obvious increase with increasing potential. So from the analyses of EIS and Tafel, reaction (2) as rate –determining step at high potential range can well explain experimental results.

Impedance spectroscopy of the electrooxidation of methanol on electrochemically polarized PtRu/C catalyst indicates that cathodic polarization leads to an enhancement for methanol oxidation. The reaction proceeds with one adsorbed intermediate of appreciable surface concentration and lifetime. The different impedance behaviors in three different potential regions reveal that the mechanism and rate-determining step in methanol electrooxidation vary with potentials. At low potential range, methanol dehydrogenation is rate-determining step while at high potential range, the oxidation and removal of CO_{ads} became rate-determining step. Meanwhile, at intermediate potential region, the rate-determining step in methanol electrooxidation is maybe in transition range.

4. Conclusions

The goal of the present study is to determine the influence of different electrochemical polarization on catalytic activity of PtRu/C catalyst to methanol electrooxidation. Moreover, kinetic parameters and rate-determining step for methanol electrooxidation were analyzed.

It has been found, in all cases, that the cathodic polarization of PtRu/C in H_2SO_4 solution at −0.30 V leads to a significant enhancement in activity for methanol electrooxidation, while anodic polarization at 0.55 V results in passivation of PtRu/C catalyst. A reasonable explanation is that the metallic state Pt^0Ru^0 can be formed during cathodic polarization and contribute to electrooxidation of methanol, while being probably, the formation of inactive Ru oxides during anodic polarization cause the blockage of dehydrogenation of methanol and subsequent oxidation removal of intermediate.

The kinetic data from Tafel plots and impedance spectroscopy of the methanol electrooxidation on electrochemically polarized PtRu/C catalyst also indicate that cathodic polarization leads to an enhancement for methanol oxidation. The reaction proceeds with one adsorbed intermediate of appreciable surface concentration and lifetime. The Tafel slope values and impedance behaviors in different potential regions reveal the mechanism and rate-determining step in methanol electrooxidation vary with potentials. At low potential range, methanol dehydrogenation is rate-determining step, while at high potential range, the oxidation and removal of CO_{ads} became rate-determining step. Meanwhile, at intermediate potential, the rate-determining step in methanol electrooxidation is maybe in transition range.

Acknowledgement

The authors wish to acknowledge the financial support of this work from Ministry of Science and Technology of China

(Grant No. G2000026408) and China Postdoctoral Science Foundation (Grant No. 2004035300).

References

[1] A.S. Aricò, V. Baglio, E. Modica, A.D. Blasi, V. Antonucci, Electrochem. Commun. 6 (2004) 164.
[2] W.H.L. Valbuena, V.A. Paganin, A.P.L. Carlos, F. Galembeck, Electrochim. Acta 48 (2003) 3869.
[3] T. Schultz, S. Zhou, K. Sundmacher, Chem. Eng. Technol. 24 (2001) 12.
[4] G. Hoogers, D. Thompsett, Catal. Tech. 3 (1999) 106.
[5] Y.X. Chen, A. Miki, S. Ye, H. Sakai, M. Osawa, J. Am. Chem. Soc. 125 (2003) 3680.
[6] Y. Zhu, H. Uchida, T. Yajima, M. Watanabe, Langmuir 17 (2001) 146.
[7] E. Herrero, W. Chrzanowski, A. Wieckowski, J. Phys. Chem. B 99 (1995) 10423.
[8] H.A. Gasteiger, N.M. Markovic, P.N. Ross Jr., J. Phys. Chem. B 99 (1995) 8945.
[9] P.K. Shen, A.C.C. Tseung, J. Electrochem. Soc. 141 (1994) 3082.
[10] S. Swathirajan, Y.M. Mikhail, J. Electroanal. Chem. 138 (1991) 1321.
[11] T. Frelink, W. Visscher, J.A.R. van Veen, Surf. Sci. 335 (1995) 353.
[12] C. Roth, N. Martz, F. Hahn, J.M. Leger, C. Lamy, H. Fuess, J. Electrochem. Soc. 149 (2002) E433.
[13] M. Watanabe, S. Motoo, J. Electroanal. Chem. 60 (1975) 267.
[14] C. Lu, C. Rice, R.I. Masel, P.K. Babu, P. Waszczuk, H.S. Kim, E. Oldfield, A. Wieckowski, J. Phys. Chem. B 106 (2002) 9581.
[15] D. Kardash, C. Korzeniewski, N. Markovic, J. Electroanal. Chem. 500 (2001) 518.
[16] D. Chu, S. Gilman, J. Electrochem. Soc. 143 (1996) 1685.
[17] B.R. Rauhe, F.R. Mclarnon, E.J. Cairns, J. Electrochem. Soc. 142 (1995) 1073.
[18] L. Dubau, F. Hahn, C. Coutanceau, J.M. Leger, C. Lamy, J. Electroanal. Chem. 554 (2003) 407.
[19] Y. Morimoto, E.B. Yeager, J. Electroanal. Chem. 444 (1998) 95.
[20] C.H. Lee, C.W. Lee, D. Kim, S.E. Bae, Int. J. Hydrogen Energy 27 (2002) 445.
[21] J.Y. Kim, Z.G. Yang, C.C. Chang, T.L. Valdez, S.R. Narayanan, P.N. Kumta, J. Electrochem. Soc. 150 (2003) 1421.
[22] T. Iwasita, H. Hoster, A.J. Anacker, W.F. Lin, W. Vielstich, Langmuir 16 (2000) 522.
[23] D.A. McKeown, P.L. Hagans, L.P.L. Carette, A.E. Russell, K.E. Swider, D.R. Rolison, J. Phys. Chem. B 103 (1999) 4825.
[24] E. Antolini, Mater. Chem. Phys. 78 (2003) 563.
[25] F. Besenbacher, I. Chorkendorff, B. Clausen, B. Hammer, A. Molenbroek, J.K. Norskov, I. Stensgaard, Science 279 (1998) 1913.
[26] Y.Y. Tong, H.S. Kim, P.K. Babu, P. Waszczuk, A. Wieckowski, E. Oldfield, J. Am. Chem. Soc. 124 (2002) 468.
[27] Q. Ge, S. Desai, M. Neurock, K. Kourtakis, J. Phys. Chem. B 105 (2001) 9533.
[28] M.S. Liao, C.R. Cabrera, Y. Ishikawa, Surf. Sci. 445 (2000) 267.
[29] R.C. Binning, M.S. Liao, C.R. Cabrera, Y. Ishikawa, H. Iddir, R. Liu, E.S. Smotkin, A. Aldykiewicz, D.J. Myers, Int. J. Quant. Chem. 77 (2000) 589.
[30] B. Gurau, R. Viswanathan, T.J. Lafrenz, R. Liu, K.L. Ley, E.S. Smotkin, E. Reddington, A. Sapienza, B.C. Chan, T.E. Mallouk, S. Sarangapani, J. Phys. Chem. B 102 (1998) 9997.
[31] D.R. Rolison, P.L. Hagans, K.E. Swider, J.W. Long, Langmuir 15 (1999) 774.
[32] J.W. Long, R.M. Stroud, K.E. Swider-Lyons, D.R. Rolison, J. Phys. Chem. B 104 (2000) 9772.
[33] A.H.C. Sirk, J.M. Hill, S.K.Y. Kung, V.I. Birss, J. Phys. Chem. B 108 (2004) 689.
[34] H. Hoster, T. Iwasita, H. Baumgartner, W. Vielstich, J. Electrochem. Soc. 148 (2001) A496.
[35] W.E. O'Grady, P.L. Hagans, K.I. Pandya, D.L. Maricle, Langmuir 17 (2001) 3047.
[36] J.O. Bockris, J. Kim, J. Electrochem. Soc. 143 (1996) 3801.
[37] R.E. Melnick, G.T.R. Palmore, J. Phys. Chem. B 105 (2001) 1012.
[38] R.E. Melnick, G.T.R. Palmore, J. Phys. Chem. B 105 (2001) 9449.
[39] J.W. Long, K.E. Swider, C.I. Merzbacher, D.R. Rolison, Langmuir 15 (1999) 780.
[40] V.L. Briss, R. Myers, H.A. Kozlowska, B.E. Conway, J. Electrochem. Soc. 131 (1984) 1502.
[41] R. Viswanathan, G. Hou, R. Liu, S.R. Bare, F. Modica, G. Mickelson, C.U. Segre, N. Leyarovska, E.S. Smotkin, J. Phys. Chem. B 106 (2002) 3458.
[42] L. Dubau, F. Hahn, C. Coutanceau, J.M. Leger, C. Lamy, J. Electroanal. Chem. 554 (2003) 407.
[43] S.L. Gojkovic, T.R. Vidakovic, D.R. Durovic, Electrochim. Acta 48 (2003) 3607.
[44] P.S. Kauranen, E. Skou, J. Munk, J. Electroanal. Chem. 404 (1996) 1.
[45] D.A. Harrington, B.E. Conway, Electrochim. Acta 32 (1987) 1703.
[46] C.N. Cao, Electrochim. Acta 35 (1990) 831.
[47] A. Maritan, Electrochim. Acta 35 (1990) 141.
[48] J.T. Muller, P.M. Urban, W.F. Holderich, J. Power Sour. 84 (1999) 157.
[49] V.S. Bagotzky, Y.B. Vassilyew, Electrochim. Acta 12 (1967) 1323.